ISSN Online: 2821-1693

Transactions on Machine Intelligence

Journal Homepage: https://tmachineintelligence.ir/index.php/TMI

Position Control of Permanent Magnet DC Motor Using IMC-Based PID Controller

N. Talebi[1,*]

[1] Department of Electrical and Computer Engineering, Yadegar-e-Imam Khomeini (RAH) Shahre Rey Branch, Islamic Azad University, Tehran, Iran

ARTICLE INFO

Article History:
Received 25 April 2021
Received in revised form 20 May 2021
Accepted 16 June 2021
Available online 17 June 2021

Keywords:
PID Controller, Position Control, Permanent Magnet DC Motor, IMC Method

ABSTRACT

The position control of permanent magnet DC motors (PMDCMs) has gained significant attention in recent years, particularly with the advent of advanced control strategies such as Internal Model Control (IMC) combined with Proportional-Integral-Derivative (PID) controllers. This literature review synthesizes various research findings that explore the effectiveness of IMC-based PID controllers for position control applications, while also identifying knowledge gaps and suggesting future research directions. Today, permanent magnet DC motors hold a significant position in theoretical and industrial applications due to their simplicity in implementation and control. PID controllers, renowned as one of the most popular controllers in the industry, continue to maintain their esteemed status. This paper aims to leverage the robust capabilities of the Internal Model Control (IMC) method to develop a PID controller to regulate the position of permanent magnet DC motors. In the proposed controller, the proportional (kP), derivative (kD), and integral (kI) gains are determined by IMC. Simulation results demonstrate that the proposed design outperforms traditionally tuned PID controllers and is capable of effectively controlling the motor position under various conditions.

1. INTRODUCTION

Permanent magnet DC motors are extensively used in various industries, such as robotics, automobiles, and air conditioning systems, owing to their precision and ease of control [1-5]. Therefore, the development of driver circuits for these motors in various applications is essential [6]. DC driver circuits are widely used in industrial applications for controlling the position and speed of DC motors due to their simplicity, ease of use, high reliability, flexibility, and cost-effectiveness [7]. Consequently, researchers have employed various methods, both classical and intelligent, to enhance efficiency, reduce complexity, and improve the accuracy of motor control. Classical methods include PID control, optimal control, and robust control, while intelligent methods are based on neural networks, evolutionary algorithms, and fuzzy logic. Additionally, hybrid approaches like fuzzy-neural solutions have been used for motor control. A significant challenge in utilizing PID controllers for DC motor control is the nonlinear

* Corresponding Author: n.talebi@live.com
Department of Electrical and Computer Engineering, Yadegar-e-Imam Khomeini (RAH) Shahre Rey Branch, Islamic Azad University, Tehran, Iran

http://dx.doi.org/10.47176/TMI.2021.90

effects inherent in these motors. Nonlinear characteristics of a DC motor, such as saturation and friction, can diminish the performance of these controllers [8], [9]. Moreover, accurately estimating the parameters of a DC motor is a tedious and complex task. Hence, approximate parameter values are used in controller design, which introduces parametric uncertainty in the motor. This uncertainty impacts the controller's performance, necessitating reconfiguration of the existing controller with parameter changes. In classical PID controllers, the controller is designed based on system parameters once and remains unchanged thereafter, implying that the proportional (kP), derivative (kD), and integral (kI) gains are fixed, thus limiting the controller's performance.

In recent years, various methods have been proposed by researchers for controlling permanent magnet DC motors, some of which are reviewed here. In [10] and [11], researchers presented a fuzzy logic-based control method for motor control. In [12], the Particle Swarm Optimization (PSO) algorithm was employed to tune the PID controller parameters. Researchers in [13] proposed a deep learning-based control method. Additionally, [14] and [15] utilized artificial neural networks for DC motor control. Reference [16] introduced a fuzzy-neural controller, and [17] discussed position control of a permanent magnet DC motor using an adaptive fuzzy PID controller.

It is evident that limited research in this field has addressed the issue of uncertainty. This paper presents a PID controller using the IMC method for controlling a DC motor. In the proposed controller, the proportional (kP), derivative (kD), and integral (kI) gains are determined by the IMC method. Simulation results analyze and evaluate the effectiveness of the proposed controller under various performance conditions.

The following sections of the paper discuss the dynamics of a permanent magnet DC motor and present the design of the IMC-based PID controller. The last section examines simulation results across different scenarios.

2. PERMANENT MAGNET DC MOTOR MODELING

This section examines the modeling of the DC motor. Figure 1 shows the equivalent circuit of this motor. Based on the equivalent circuit in Figure 1, the following electrical equation governs the motor:

$$V = Ri + L\frac{di}{dt} + E \tag{1}$$

where R is the armature resistance, L is the armature inductance, and E is the back electromotive force (EMF). In the mechanical part of the motor, the following relation holds:

$$J\ddot{\theta} + B\dot{\theta} + T_l = T \tag{2}$$

In the above relation, T is the motor torque, J is the armature inertia, B is the armature damping coefficient, T_l is the load torque, θ is the angle, $\dot{\theta}$ is the angular velocity, and $\ddot{\theta}$ is the angular acceleration. Additionally, we have:

$$T = K_m i \tag{3}$$

$$E = K_b\dot{\theta} \tag{4}$$

where K_m is the torque constant, and K_b is the back EMF constant. By taking the Laplace transform of relations (1) to (4), the transfer function of the motor from the input voltage to the angular position output can be found.

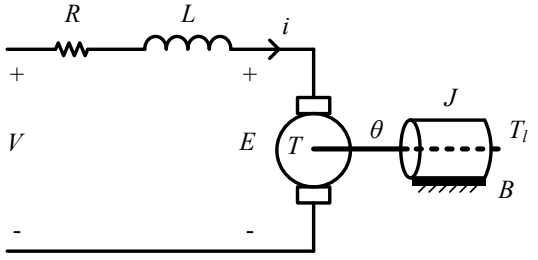

Fig.1. Equivalent Circuit of Permanent Magnet DC Motor.

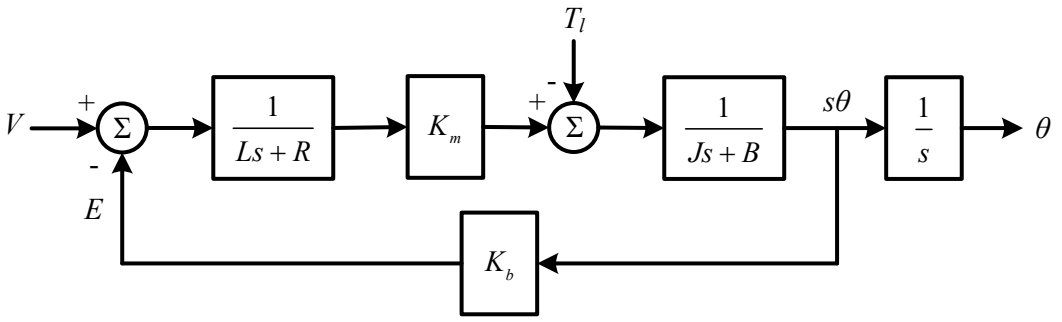

Fig.2. Block Diagram of Permanent Magnet DC Motor.

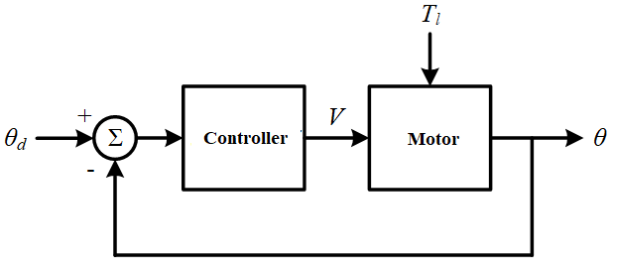

Fig.3. Closed-Loop System for Position Control of Permanent Magnet DC Motor.

The block diagram in Figure 2 represents the DC motor model in the Laplace domain. Since the motor is controlled by voltage, the controller must determine the motor's input voltage to achieve the desired angular position. Figure 3 illustrates the closed-loop system for the position control of a permanent magnet DC motor.

3. CONTROLLER DESIGN

In this section, the IMC-based PID controller is designed. First, the IMC method for second-order systems is described, and then it is applied to the permanent magnet DC motor. Consider the following second-order system:

$$\tilde{g}_p(s) = \frac{k}{(\tau_1 s+1)(\tau_2 s+1)} \tag{5}$$

In the first step, the IMC controller transfer function is found. At this stage, q(s) is allowed to be improper since the ultimate goal is to obtain a PID controller. Hence, we have:

$$q(s) = \tilde{q}(s)f(s) = \tilde{g}_p^{-1}(s)f(s) = \frac{(\tau_1 s+1)(\tau_2 s+1)}{k}\frac{1}{(\lambda s+1)} \tag{6}$$

where f(s) is the filter associated with the IMC controller, with the adjustable parameter λ.

In the second step, the equivalent standard feedback controller is found using the following relation:

$$g_c(s) = \frac{q(s)}{1-\tilde{g}_p(s)q(s)} = \frac{\frac{(\tau_1 s+1)(\tau_2 s+1)}{k(\lambda s+1)}}{1-\frac{k}{(\tau_1 s+1)(\tau_2 s+1)}\frac{(\tau_1 s+1)(\tau_2 s+1)}{k(\lambda s+1)}} = \frac{\tau_1\tau_2 s^2+(\tau_1+\tau_2)s+1}{k\lambda s} \tag{7}$$

Now, considering the PID controller transfer function shown below, the next step can be executed:

$$g_c(s) = k_c\left(\frac{\tau_I\tau_D s^2 + \tau_I s + 1}{\tau_I s}\right) \tag{8}$$

In the third step, to convert relation (7) into the PID controller transfer function form (8), we multiply both the numerator and denominator of relation τ1+ τ2. Consequently, we have:

$$g_c(s) = \left(\frac{\tau_1 + \tau_2}{k\lambda}\right)\frac{\tau_1\tau_2 s^2 + (\tau_1 + \tau_2)s + 1}{(\tau_1 + \tau_2)s} \tag{9}$$

By comparing relations (8) and (9), the PID controller gains are obtained as follows:

$$\begin{aligned} k_c &= \frac{\tau_1 + \tau_2}{k\lambda} \\ \tau_I &= \tau_1 + \tau_2 \\ \tau_D &= \frac{\tau_1\tau_2}{\tau_1 + \tau_2} \end{aligned} \tag{10}$$

It is noteworthy that the PID controller gains in the parallel structure can be determined using the following relations:

$$\begin{aligned} k_p &= k_c \\ k_I &= \frac{k_c}{\tau_I} \\ k_D &= k_c\tau_D \end{aligned} \tag{11}$$

As shown in relations (5) to (11), to determine the PID controller gains using the IMC method, the system transfer function is required. Therefore, considering Figure 2, the transfer function of the permanent magnet DC motor from the input voltage to the angular position output is obtained as follows:

$$\begin{aligned} &\frac{\theta}{V} = \frac{\dfrac{K_m}{Ls+R}\dfrac{1}{Js+B}}{1 + \dfrac{K_m}{Ls+R}\dfrac{1}{Js+B}K_b} \times \frac{1}{s} = \frac{K_m}{(Ls+R)(Js+B) + K_mK_b} \times \frac{1}{s} \\ &\rightarrow \frac{\theta}{V} = \frac{K_m}{s(LJs^2 + (LB+RJ)s + RB + K_mK_b)} \end{aligned} \tag{12}$$

It is clear from relation (12) that the system is of third order. To apply the IMC method, assuming the armature inductance is approximately zero (common in position control discussions of permanent magnet DC motors, especially in robotics control applications), relation (12) is simplified as follows:

$$\frac{\theta}{V} \approx \frac{K_m}{s(RJs + RB + K_mK_b)} \tag{13}$$

Rewriting relation (13) into the form of relation (5), we have:

$$\frac{\theta}{V} \approx \frac{\dfrac{K_m}{RB + K_m K_b}}{s\left(\dfrac{RJ}{RB + K_m K_b} s + 1\right)} \rightarrow \begin{cases} k = \dfrac{K_m}{RB + K_m K_b} \\ \tau_1 = 1 \\ \tau_2 = \dfrac{RJ}{RB + K_m K_b} \end{cases} \tag{14}$$

Thus, with the system parameters determined based on relation (14), the PID controller gains can be obtained using relation (10) as follows:

$$\begin{aligned} k_c &= \frac{1 + \dfrac{RJ}{RB + K_m K_b}}{\dfrac{K_m}{RB + K_m K_b} \lambda} \\ \tau_I &= 1 + \frac{RJ}{RB + K_m K_b} \\ \tau_D &= \frac{\dfrac{RJ}{RB + K_m K_b}}{1 + \dfrac{RJ}{RB + K_m K_b}} \end{aligned} \tag{15}$$

This completes the design process of the IMC-based PID controller. It is noteworthy that in this research, the PID controller is designed based on frequency response to compare the performance of the proposed design with it. The gains of this controller are provided in the appendix.

4. SIMULATION AND ANALYSIS OF RESULTS

As previously mentioned, various scenarios were employed to evaluate the performance of the proposed control system in this study. The system parameter values used in the simulation are compiled in the appendix. Notably, all simulations were conducted using MATLAB version R2008a in the Simulink environment.

Initially, to determine the appropriate value for the IMC filter parameter, λ, several simulations were performed with a fixed input of one radian, in the absence of disturbances and uncertainties. The simulation results are shown in Figure 4. As illustrated, increasing this parameter reduces response speed, increases steady-state error, and amplifies maximum overshoot. Based on Figure 4, a value of 0.01 was chosen for the filter parameter and is utilized in the scenarios discussed in this section.

Scenario 1: Setpoint Tracking

In this scenario, the motor position reference was set to one radian, and the results were observed in the presence and absence of disturbances (specifically, load torque). The angular position of the motor and the error signal in this scenario are depicted in Figures 5 and 6. As shown, the proposed controller exhibits satisfactory performance with minimal error. Additionally, system performance metrics during transient states, such as rise time, settling time, and maximum overshoot, are appropriate.

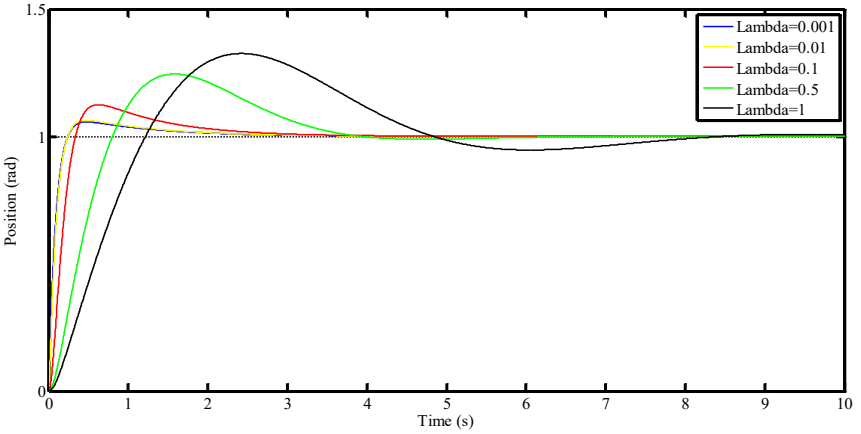

Fig.4. Motor Angular Position for Various λ Values with a Reference of One Radian

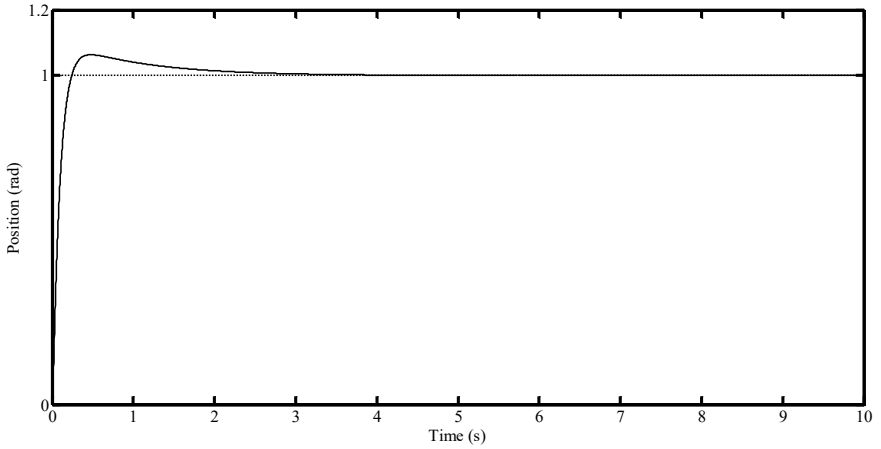

Fig.5. Motor Angular Position with a Reference of One Radian

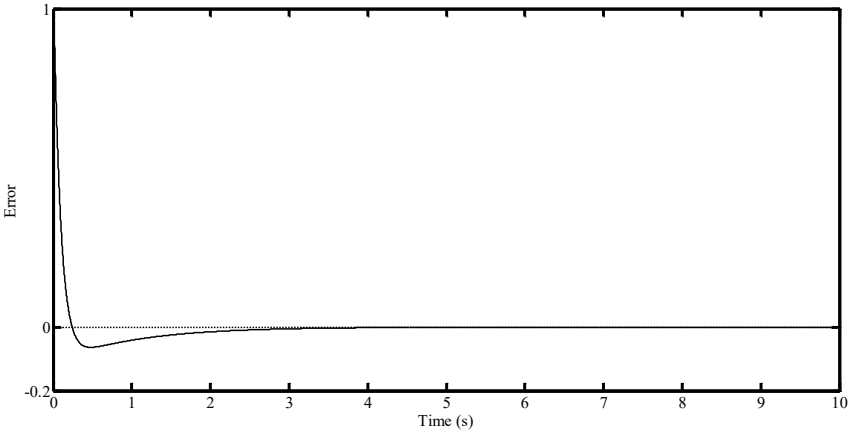

Fig.6. Error Signal with a Reference of One Radian

To further assess the performance of the designed controller, a disturbance signal with an amplitude of 5% of the final value was applied as load torque to the motor at the fifth second of the simulation. The simulation results, comparing the performance of the proposed controller with a frequency response-based tuned controller, are shown in Figure 7. As indicated, after the load torque is applied at the fifth second, some oscillations in the angular position are observed, resulting in a maximum error amplitude of 0.3595, which is damped out within approximately 3 seconds. Therefore, based on the simulation results in this scenario, it can be concluded that the proposed structure exhibits satisfactory performance (in terms of transient and steady-state behavior) in setpoint tracking and under disturbance conditions.

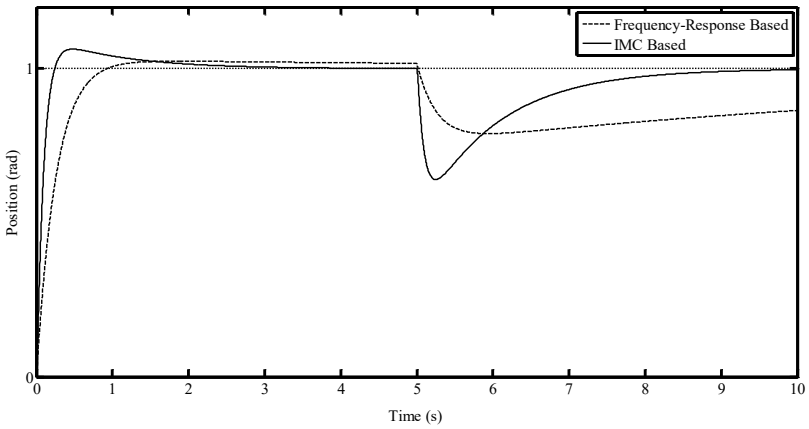

Fig.7. Comparison of the Performance of Two Controllers for a Reference of One Radian under Disturbance Conditions

Scenario 2: Position Tracking

In the second scenario, the control system's performance was evaluated for a time-varying desired position. A fixed input of one radian was applied from the beginning of the simulation until the fifth second, followed by a constant positive slope input from the fifth to the tenth second, a fixed input of six radians from the tenth to the fifteenth second, and a constant negative slope input from the fifteenth to the twentieth second. Additionally, a 5% disturbance was applied to the system at the eighth second. The simulation results for this scenario are shown in Figure 8. The results indicate that the proposed control system performs well in position tracking, with minimal tracking error. Oscillations observed at the fifth, eighth, tenth, and fifteenth seconds are due to input changes and disturbances, with transient states quickly damped by the control system. The system's behavior in this scenario also exhibits desirable transient and steady-state characteristics, effectively mitigating disturbances.

Scenario 3: Parameter Uncertainty Analysis

In the final scenario, the presence of uncertainties in motor parameters was investigated. Specifically, the parameter R was decreased by 20% from its nominal value, L was increased by 10%, B was decreased by 10%, and J was increased by 30%. The nominal values of these parameters are provided in the appendix. It is noteworthy that a constant input was considered in this scenario, and no disturbance was applied to the system. The simulation results for this scenario are shown in Figure 9. Despite the changes in system parameters, the control system continues to perform satisfactorily, demonstrating the proposed control system's adaptability to parameter variations. From Figure 9, it can be seen that the maximum overshoot is six percent, and the rise time is less than 0.23 seconds, with very minimal steady-state error.

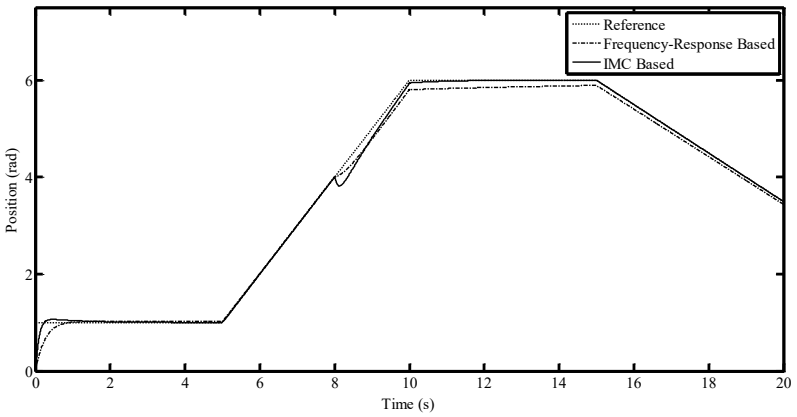

Fig.8. Comparison of the Performance of Two Controllers for Time-Varying Input and Disturbance Conditions

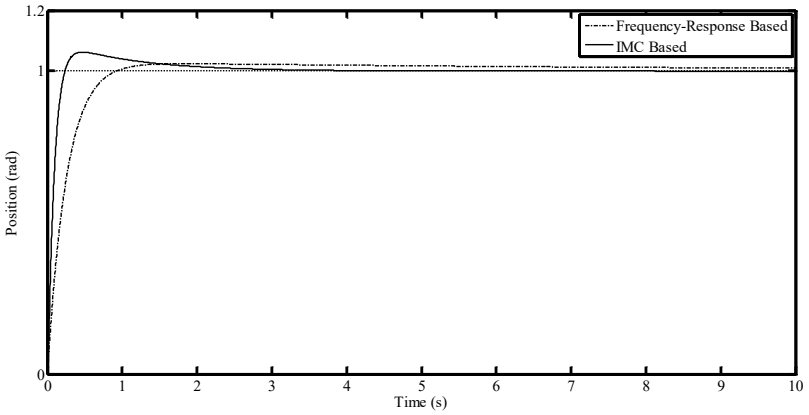

Fig.9. Comparison of the Performance of Two Controllers with a Reference of One Radian and Parameter Uncertainties

5. CONCLUSION

This paper presented a PID control system based on the Internal Model Control (IMC) method for controlling the position of a permanent magnet DC motor. In the proposed controller structure, the proportional, integral, and derivative gains of the PID controller were determined using the IMC method. To evaluate the proposed system's performance, a frequency response-based PID controller was also designed. Simulation results across three different scenarios demonstrated that the proposed control system offers satisfactory transient and steady-state behavior. The proposed control system exhibits desirable performance for both fixed and time-varying inputs, under disturbance conditions, and with parameter uncertainties.

6. APPENDIX

PID Controller Parameters Tuned Based on Frequency Response

$k_p = 20.46, k_I = 2.31, k_D = 5.02.$

DC Motor Parameters

$R = 1\ \Omega$, $L = 0.001\ H, J = 0.0001\ kgm^2$, $B = 0.001\ Nm / rad / s$, $K_m = K_b = 0.01.$

Transparency Statement

The data supporting this study are available upon reasonable request to the corresponding author, subject to ethical and confidentiality considerations.

Acknowledgments

We would like to express our gratitude to all individuals who contributed to this project.

Declaration of Interest

The authors declare that they have no competing interests.

Funding

This research received no specific grant from any funding agency, commercial, or not-for-profit sectors.

REFERENCES

[1] Tong, W., Li, S., Pan, X., Wu, S., & Tang, R. (2020). Analytical model for cogging torque calculation in surface-mounted permanent magnet motors with rotor eccentricity and magnet defects. *IEEE Transactions on Energy Conversion, 35*, 2191-2200. https://doi.org/10.1109/TEC.2020.2995902

[2] De Klerk, M. L., & Saha, A. (2021). A comprehensive review of advanced traction motor control techniques suitable for electric vehicle applications. *IEEE Access, 9*, 125080-125108. https://doi.org/10.1109/ACCESS.2021.3110736

[3] Wang, M., Sun, D., Ke, W., & Nian, H. (2021). A universal lookup table-based direct torque control for OW-PMSM drives. *IEEE Transactions on Power Electronics, 36*, 6188-6191. https://doi.org/10.1109/TPEL.2020.3037202

[4] Xu, J., Du, Y., Fang, H., Guo, H., & Chen, Y. (2020). A robust observer and nonorthogonal PLL-based sensorless control for fault-tolerant permanent magnet motor with guaranteed postfault performance. *IEEE Transactions on Industrial Electronics, 67*, 5959-5970. https://doi.org/10.1109/TIE.2019.2931235

[5] Poudel, B., Amiri, E., Rastgoufard, P., & Mirafzal, B. (2021). Toward less rare-earth permanent magnet in electric machines: A review. *IEEE Transactions on Magnetics, 57*, 1-19. https://doi.org/10.1109/TMAG.2021.3095615

[6] Mayank, J. N. R., & Nandwani, S. M. (2012). Speed control of DC motor using fuzzy logic technique. *IOSR Journal of Electrical and Electronics Engineering, 3*(6), 41-48. https://doi.org/10.9790/1676-0364148

[7] Bansal, U. K., & Narvey, R. (2013). Speed control of DC motor using fuzzy PID controller. *Advance in Electronic and Electric Engineering, 3*(9), 1209-1220.

[8] Johnson, C. T., & Lorenz, R. D. (1992). Experimental identification of friction and its compensation in precise, position controlled mechanism. *IEEE Transactions on Industrial Applications, 28*(6). https://doi.org/10.1109/28.175293

[9] Chalmers, B. J. (1992). Influence of saturation in brushless permanent magnet drives. *IEE Proceedings B*

(Electric Power Applications), 139(1). https://doi.org/10.1049/ip-b.1992.0007

[10] Ismail, N. L., Zakaria, K. A., Moh Nazar, N. S., Syaripuddin, M., Mokhtar, A. S. N., & Thanakodi, S. (2017). DC motor speed control using fuzzy logic controller. *International Conference on Engineering and Technology (IntCET 2017)*, 1-6. https://doi.org/10.1063/1.5022920

[11] Dökmetaş, B., Akçam, N., & Faris, M. (2016). Speed control of DC motor using fuzzy logic application. *4th International Symposium on Innovative Technologies in Engineering and Science*, 734-740.

[12] Kaushal, A., Thakur, N., & Nagaria, D. (2014). Comparison of speed control of DC motor using fuzzy-PID and PSO-PID technique. *International Journal of Information & Computation Technology, 4*(6), 553-558.

[13] Cheon, K., Kim, J., Hamadache, M., & Lee, D. (2015). On replacing PID controller with deep learning controller for DC motor system. *Journal of Automation and Control Engineering, 3*(6), 452-456. https://doi.org/10.12720/joace.3.6.452-456

[14] Brandstetter, P. (2014). Sensorless control of DC drive using artificial neural network. *Acta Polytechnica Hungarica, 11*(10), 5-20. https://doi.org/10.12700/APH.11.10.2014.10.1

[15] Talib, J. G. (2016). Modelling and control of DC motor using neural networks. *International Journal of Computer Science and Mobile Computing, 5*(5), 803-807.

[16] Premkumar, K., & Manikandan, B. V. (2014). Adaptive neuro-fuzzy inference system based speed controller for brushless DC motor. *Neurocomputing, 138*, 260-270. https://doi.org/10.1016/j.neucom.2014.01.038

[17] Talebi, N. (2019). Position control of permanent magnet DC motor using adaptive fuzzy PID controller. *5th National Conference on Knowledge and Technology of Mechanical and Electrical Engineering of Iran*, Tehran, September 2019.